ISSN 0021-3640, JETP Letters, 2009, Vol. 90, No. 4, pp. 272–277. © Pleiades Publishing, Ltd., 2009.
Original Russian Text © A.A. Eliseev, D.F. Gorozhankin, K.S. Napolskii, A.V. Petukhov, N.A. Sapoletova, A.V. Vasilieva, N.A. Grigoryeva, A.A. Mistonov, D.V. Byelov, W.G. Bouwman, K.O. Kvashnina, D.Yu. Chernyshov, A.A. Bosak, S.V. Grigoriev, 2009, published in Pis'ma v Zhurnal Éksperimental'noĭ i Teoreticheskoĭ Fiziki, 2009, Vol. 90, No. 4, pp. 297–303.

Determination of the Real Structure of Artificial and Natural Opals on the Basis of Three-Dimensional Reconstructions of Reciprocal Space

A. A. Eliseev[a], D. F. Gorozhankin[a], K. S. Napolskii[a, *], A. V. Petukhov[b], N. A. Sapoletova[a], A. V. Vasilieva[c], N. A. Grigoryeva[d], A. A. Mistonov[d], D. V. Byelov[b], W. G. Bouwman[e], K. O. Kvashnina[f], D. Yu. Chernyshov[d, g], A. A. Bosak[f], and S. V. Grigoriev[c]

[a] *Faculty of Materials Science, Moscow State University, Moscow, 119991 Russia*

* *e-mail: napolsky@inorg.chem.msu.ru*

[b] *Debye Institute for Nanomaterials, University of Utrecht, 3584 CH Utrecht, The Netherlands*

[c] *Petersburg Nuclear Physics Institute, Russian Academy of Sciences, Gatchina, 188308 Russia*

[d] *St. Petersburg State University, St. Petersburg, 198504 Russia*

[e] *Delft University of Technology, 2629 JB Delft, The Netherlands*

[f] *European Synchrotron Radiation Facility, BP220, F-38043 Grenoble Cedex, France*

[g] *Swiss–Norwegian Beam Lines at the European Synchrotron Radiation Facility, BP220, F-38043 Grenoble Cedex, France*

Received June 25, 2009

The distribution of the scattering intensity in the reciprocal space for natural and artificial opals has been reconstructed from a set of small-angle X-ray diffraction patterns. The resulting three-dimensional intensity maps are used to analyze the defect structure of opals. The structure of artificial opals can be satisfactorily described in the Wilson probability model with the prevalence of layers in the fcc environment. The diffraction patterns observed for a natural opal confirm the presence of sufficiently long unequally occupied fcc domains.

PACS numbers: 61.05.Cf, 61.72.Dd, 64.75.Yz

DOI: 10.1134/S0021364009160103

INTRODUCTION

Opal is one of the widely known jewellery stones, which attracts attention owing to playing of colors and striking colorblends. Its name descends from the Greek word *opállios* (precious stone) [1]. It is accepted that opal has been known since 250 BC, but its structure was determined using light diffraction [2–4] and electron microscopy [5] not too long ago, less than 50 years ago. The interest in the investigation of opals and methods of their artificial formation has been refreshed in the last two decades. This interest is stimulated by the appearance and development of photonics, which is a scientific field studying the possibility of controlling flow of light. Photonic crystals are among materials promising for photonics; their structure is characterized by a strictly periodic variation of the refractive index at scales comparable with the wavelength of electromagnetic radiation [6, 7]. The main property of photonic crystals is that the spectra of their electromagnetic eigenstates include photonic band gaps within which the propagation of electromagnetic radiation is suppressed in all of the crystallographic directions or in some of them [8]. Photonic crystals are often considered as optical analogs of semiconductor materials. Photonic crystals are of applied interest for creating optical filters, ultrafast switchers, amplifiers, and high-efficiency emitters.

Natural opals are formed in the Earth's interior from spherical silicon oxide particles close in size under the conditions of not too high temperatures and pressures in the presence of gravity. Artificial opals, which are colloidal crystals, are most often obtained by the methods of self-assembly of submicron spherical particles of silicon oxide, polystyrene, or polymethyl methacrylate under the action of gravitational, capillary, convective, and electrostatic forces [9–12].

It is convenient to consider colloidal crystals consisting of spherical particles in terms of the closest packed structures consisting of hexagonal close packed layers; each of them can occupy one of three nonequivalent positions A, B, or C. The structure of a colloidal crystal is determined by the sequence of the packing of such layers. The three-layer stacking *ABCABC* (or *ACBACB*) corresponds to the fcc lattice. The sequence *ABABAB* corresponds to the hexagonal close-packed structure. The arbitrary alternation of

layers is considered in terms of the formation of a random hexagonal close-packed structure. When film samples of artificial opals are formed, hexagonal layers of microspheres are arranged in parallel to the substrate. It is commonly accepted that the vertical deposition method often leads to the formation of photonic crystals with the fcc structure [13, 14], although information on their imperfection is incomplete. The aim of this work is to reveal differences and similarities in the structures of artificial and natural opals. This information is necessary both for the efficient synthesis of photonic crystals and for the reconstruction of geophysical processes accompanying the formation of natural opals.

The methods of scanning electron and scanning probe microscopies [12, 13, 15] and confocal microscopy [13, 16, 17] are widely used for investigating materials ordered at the nano and submicron levels. In addition to obvious advantages such as availability and high resolution, these methods have a serious disadvantage—locality and, therefore, very limited statistics of the obtained information. At the qualitative level, the structure of photonic crystals can be studied using optical spectroscopy. In [18, 19], it was noted that the characteristic minimum in the transmission spectra or the maximum in the absorption spectra corresponding to the stopband along the $\langle 111 \rangle$ direction becomes less pronounced and wider with an increase in the number of defects in a colloidal crystal with the fcc structure. A quantitative investigation of the long-range order of the spatially ordered materials is possible only with diffraction methods, which provide information averaged over the sample volume [20, 21]. In this work, a complex investigation of a natural Australian opal and a film sample of a synthetic photonic crystal consisting of monodisperse polystyrene microspheres was performed using small-angle X-ray diffraction. To determine the real structure of the objects for small-angle diffraction experiments, we carried out the three-dimensional reconstruction of the reciprocal space. This approach is universal and applicable for a quantitative analysis of the structure of many spatially ordered materials. The methods based on the three-dimensional reconstruction of the reciprocal space from the diffraction data for analyzing the defect structure of crystalline materials were described well in [22, 23].

EXPERIMENTAL PROCEDURE

A commercially available Australian opal was used as a natural photonic crystal. The plate sample had a size of ~5 × 7 mm and a thickness of ~200 μm.

The vertical deposition method [10, 11, 13] was used to form an artificial opal. The synthesis of monodisperse microspheres is the first step of this method for obtaining photonic crystals. Their size determines the periodicity of the structure of the colloidal crystal and, as a result, the position of the photonic band gap in the energy spectrum, whereas the monodispersivity of the particles is one of the key factors determining the possibility of the self-assembly of particles into ordered clusters. A suspension of monodisperse microspheres was obtained by the polymerization of styrene in the presence of potassium persulfate as an initiator [24]. Immediately before the synthesis, styrene was purified from a polymerization inhibitor by vacuum distillation. The reaction mixture consisting of styrene, potassium persulfate, and distilled water in the molar ratio 1 C_8H_8 : 0.003 $K_2S_2O_8$: 58 H_2O was vigorously stirred on a magnetic stirrer for 24 h at a temperature of 70°C. Then, the suspension was centrifuged and the obtained white sediment was dispersed in distilled water under sonication. According to the dynamic light scattering and scanning electron microscopy, the mean diameter of the obtained particles was 530 nm and the standard deviation was no more than 5%.

The deposition of polystyrene microspheres on vertically mounted substrates of mica plates with a deposited 100- to 200-nm gold layer was performed from a ~0.2 vol % aqueous suspension at a temperature of (60 ± 3)°C. The width of the resulting photonic crystal is determined by a substrate width of 1.5 cm, whereas the film length under the assumption of a constant rate of solvent evaporation from the reaction mixture is proportional to the thermostating time. The duration of the deposition of microspheres was ~24 h, which corresponded to the formation of films 2 cm in length.

The experiments on the small-angle X-ray diffraction were carried out at the BM26B DUBBLE Dutch–Belgian beamline at the European Synchrotron Radiation Facility (Grenoble Cedex, France). We used a setup for small-angle diffraction with focusing elements, which is similar to that described in [21]. This scheme is well applicable for the diffraction analysis of periodic structures with a large period and makes it possible to reach an angular resolution of ~5–10 μrad.

In this work, the wavelength of X-rays was $\lambda = 1.01$ Å, monochromaticity was $\Delta\lambda/\lambda = 2 \times 10^{-4}$, and the beam cross section on the sample was 0.5 × 0.5 mm. The X-ray beam was focused by means of beryllium refractive optics [25]. The lenses were mounted immediately in front of the sample and focused the X-rays on a luminescent screen of a two-coordinate CCD detector (Photonic Science, resolution of 4000 × 2700 points with a size of 22 × 22 μm), which was placed at a distance of 8 m behind the sample.

The samples were mounted on a goniometer and were adjusted so that the X-ray beam was incident on the same part of a crystal rotating about the vertical axis (angle ω). To reconstruct the three-dimensional pattern of the reciprocal space, series of diffraction patterns were recorded with a step of 1° in the ranges

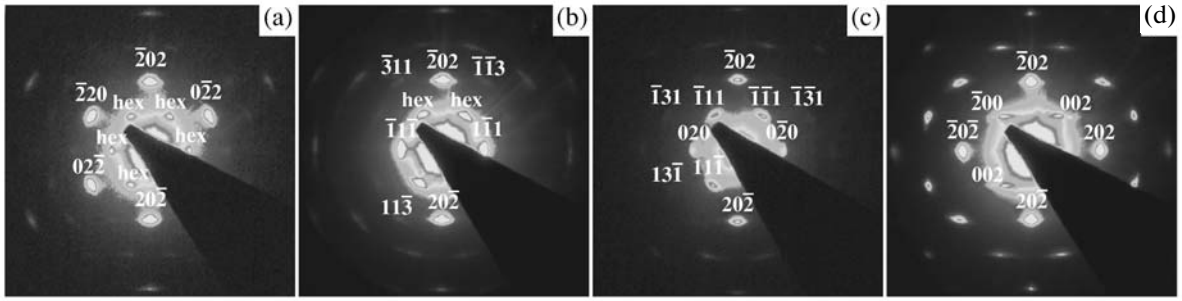

Fig. 1. Data of the small-angle X-ray diffraction for an artificial opal for the angles of incidence (a) 0°, (b) 19.5°, (c) −35.3°, and (d) 54.7°. The reflections are classified for the fcc structure. The reflections that cannot be attributed to the fcc structure are marked as hex.

$-75° < \omega < 75°$ and $-85° < \omega < 85°$ for the natural and artificial opals, respectively. Zero angle ω corresponds to the normal incidence of X rays on the plane of the samples. The exposition time was 30 s for each diffraction map. The three-dimensional reconstruction of the reciprocal space from the set of diffraction patterns obtained for various angles of the incidence of X rays on the sample was performed using a specially developed module 3D-RRS for MathCad.

RESULTS AND DISCUSSION

Figure 1 shows the diffraction patterns of an artificial opal for the characteristic angles of incidence of X rays on the sample plane: 0°, 19.5°, −35.3°, and 54.7° (corresponding to the ⟨111⟩, ⟨121⟩, ⟨101⟩, and ⟨010⟩ zones for the fcc structure, the rotation axis coincides with the $\langle 10\bar{1} \rangle$ axis of the sample). The majority of the observed reflections can be attributed to one of the twins of the fcc packing: sequences *ABCABC* or *ACBACB*.

Note that in addition to the reflections corresponding to the integer indices of the fcc lattice with a period of $a_0 = 750$ nm, the X-ray diffraction patterns contain reflections (marked as hex in Figs. 1a, 1b) that cannot appear in the ideal fcc structure. These reflections can be real Bragg reflections (e.g., corresponding to the other coexisting types of the structures) or the cross sections of long diffuse objects in the reciprocal space. The scattering pattern indicates the existence of, in the former case, some amount of the hexagonal phase in the sample and, in the latter case, stacking faults and/or a finite thickness of the samples under investigation.

When a defective structure is formed with the violation of the alternation of planar layers consisting of close-packed spheres, long rods should be observed in the reciprocal space; the intensity distribution along such diffuse objects characterizes the implemented structure [26]. Note that several cross sections of the reciprocal space are generally insufficient for the complete description of the intensity distribution along such diffuse rods.

In this work, we performed the three-dimensional reconstruction of the reciprocal space for small-angle diffraction experiments. To reconstruct the total reciprocal space, a program for the three-dimensional reconstruction of an object from a set of its two-dimensional cross sections was developed in the MathCad worksheet. The Ewald sphere in the reconstruction region can be considered as planar for the case of small-angle scattering.

The set of the initial data consists of (i) diffraction maxima located at the sites of the reciprocal lattice, (ii) diffuse rods due to the stacking faults of microspheres, and (iii) small-angle diffuse background with a maximum at $q = 0$, which is determined by the scattering of X rays on the imperfections of the sample structures and on the elements of the optical scheme. Since the intensity of the diffuse rods is low, the correct subtraction of the background is an important task determining the possibility of the correct quantitative reconstruction of the reciprocal space pattern. The background scattering is well described by the function $1/(q^2 + \zeta^2)$, where q is the scattering vector and $1/\zeta$ is the correlation length, which generally depends on the radiation coherence length, the size of the coherent scattering region of the crystal, and the form factor of the object under investigation [27]. Since the opals under investigation were plates, the spherical symmetry of the background signal was broken. The desired signal was separated from the experimental data by the subtraction of the diffuse background function (separately for each of the diffraction images). It was found that the best approximation of the background is provided by a power law of q ($I_{bg}(q)$), which depends on the polar angle and has elliptic contours. The model of the background signal was constructed in sectors of each of the diffraction images with an angular width of 5° in the polar coordinates.

The function $I_{bg}(q)$ for each sector had the form

$$I_{bg}(q) = kq^{-n} + I_{detector}, \quad (1)$$

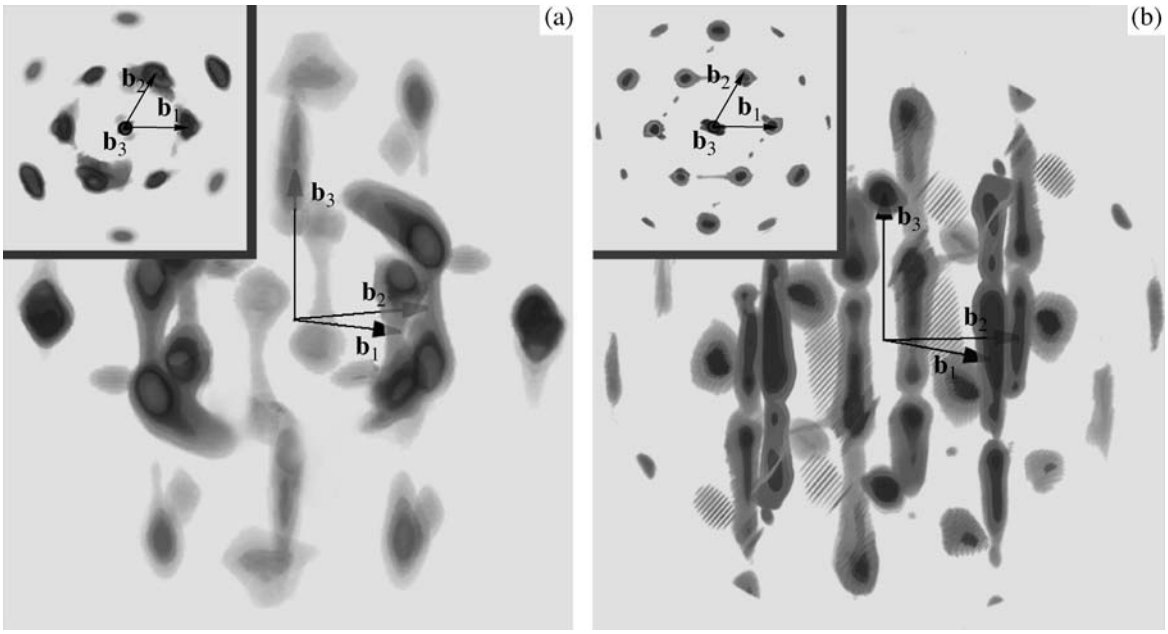

Fig. 2. Three-dimensional reconstruction of the reciprocal space for the (a) artificial and (b) natural opal samples. The basis vectors $\mathbf{b}_1$, $\mathbf{b}_2$, and $\mathbf{b}_3$ are shown in the figure. The insets show the plan view (along the vector $\mathbf{b}_3$) of the reciprocal space.

where $n = 2 + \delta$ ($\delta \ll 1$), k and n are constants in each sector, and I_{detector} is the background signal of the detector, which is a constant. When determining $I_{\text{bg}}(q)$, the points belonging to the diffraction reflections were temporarily removed from the diffraction data (the maxima were found automatically by the extrema of the derivative $\partial(Iq^2)/\partial q$, because the background is characterized by the relation $\partial((I_{\text{bg}} - I_{\text{detector}})q^2)/\partial q \approx 0$). After the construction of the background signal matrix, the two-dimensional smoothing of the diffuse background function was performed.

Owing to this algorithm, not only diffraction maxima, but also diffuse objects responsible for the stacking faults of microspheres were separated from the experimental data with the almost complete exclusion of the small-angle diffuse component. The results were used to determine the total intensity distribution along the Bragg rods.

The patterns of the reconstructed reciprocal space for the natural opal and synthetic photonic crystal are shown in Fig. 2 in the hexagonal basis specified by the vectors $\mathbf{b}_1$, $\mathbf{b}_2$, and $\mathbf{b}_3$, where $|b_1| = |b_2| = 4\pi/(\sqrt{3}\,D)$, $|b_3| = \pi\sqrt{6}\,/D$, and D is the diameter of the microspheres. First, we point to the presence of six sufficiently intense long diffuse rods of the $\{10\xi\}$ type, which are parallel to $\langle 001\rangle$. The cross section of these rods by the Ewald sphere was observed in the form of additional spots, which do not correspond to the fcc structure and are marked as hex in Fig. 1.

As mentioned above, the appearance of diffuse rods indicates the presence of planar stacking faults of the hexagonal layers in the structure of the studied photonic crystals and/or is attributed to the finite thickness of the samples. As expected, the violations of the alternation of the layers are manifested only for the reflections with $(h - k) = 3n \pm 1$ [26, 28]. The reflections of the $(h - k) = 3n$ family, which are independent of the presence of stacking faults, do not exhibit noticeable broadening associated with the form factor of the sample (see Fig. 2). Thus, the structure of the natural opal, as well as the synthetic photonic crystal obtained by the vertical deposition method, cannot be described in terms of the perfect fcc or hexagonal close packings. Note that diffuse scattering along other directions is observed in both cases in addition to rods located along the vector $\mathbf{b}_3$. This diffuse scattering component is naturally attributed to planar faults oriented at an angle of 70.5° with respect to the stacking faults discussed in detail above.

To quantitatively describe opal-like defective structures, it is convenient to use the Wilson model [26, 29], which allows for the determination of the probability of finding a layer in the fcc or hcp environment from the analysis of the intensity distribution along the diffuse rods. The main parameter in this theory is the probability α that the nth and $(n + 2)$th layers of the close-packed microspheres are not identical. The extreme α values 0 and 1 correspond to the hcp and twinned fcc structures, respectively. Intermediate values correspond to a random hexagonal close-packed structure.

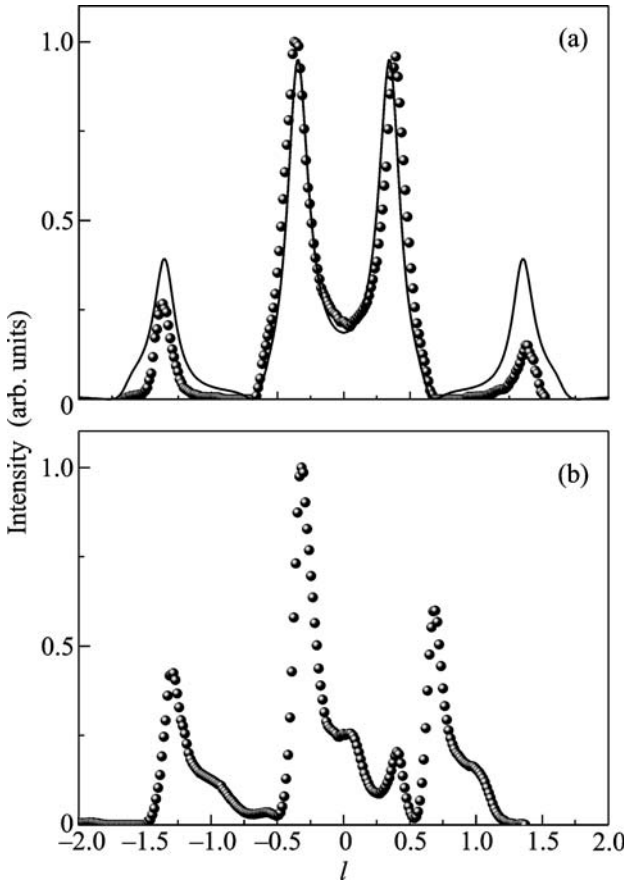

Fig. 3. Profiles of the intensity distribution along the first-order rods for the (a) artificial and (b) natural opal samples. The solid line in panel (a) corresponds to the theoretical calculation in the Wilson model with $\alpha = 0.65$.

The intensity distribution along the first-order rods was determined by the numerical integration of the experimental data (see Fig. 3). For the synthetic photonic crystal, the intensity is symmetrically distributed with respect to zero and the maxima at $l = \pm 0.37$ and ± 1.37 are pronounced. The theoretical calculation of the intensity in the Wilson model with $\alpha = 0.65$ taking into account the form factor of spherical particles is shown by the solid line in Fig. 3a. The satisfactory agreement between the experimental data and theoretical calculation allows for the statement that each layer of microspheres in the artificial opal under investigation is in the fcc environment with a probability of ~65%.

Analyzing the intensity distribution along the diffuse rods for the natural opal, we first point to the presence of the intense maxima at $l \approx -1.3$, -0.3, and 0.7 in agreement with the presence of sufficiently long *unequally occupied* fcc domains. It is known that the prevalence of one type of the fcc packing of the layers for any initial layer configuration can be achieved due to the uniaxial plastic deformation of the shift, leading to the slip of the layers [30–33]. Therefore, shear strains appear in the process of the formation of the natural opal. On the contrary, the mechanical strains of the crystal are excluded when the artificial opal is synthesized by the vertical deposition method and we observed the formation of the random hexagonal closest packing in which the blocks with two equivalent configurations of the fcc structure are formed with the same probability. The asphericity of the natural opal particles [2] significantly affects the intensity distribution along the diffuse rods and should be necessarily taken into account in a quantitative analysis. A detailed pattern of the spatial distribution of the layers in the natural opal can be obtained only when simulating packings corresponding to the experimentally observed diffuse scattering. However, such calculations are beyond the scope of this work.

CONCLUSIONS

The method proposed for analyzing the data of the small-angle X-ray diffraction provides a number of conclusions on the structure of natural and artificial opals. In both cases, the structure is the random hexagonal closest packing of microspheres. The structure of the synthetic photonic crystals obtained by the vertical deposition method can be satisfactorily described in the Wilson probability model with the prevalence of layers in the fcc environment. The diffraction pattern observed for the natural opal is consistent with the presence of sufficiently long unequally occupied fcc domains, which is apparently caused by the external forces in the crystal formation process.

The above three-dimensional reconstruction of the reciprocal space is likely the most complete characteristic of the structure of colloidal crystals. This method is universal and can be used, e.g., to investigate the structure of the superlattices of nanoparticles and arrays of quantum dots or heterostructures.

We are grateful to the staff of the BM26B DUBBLE beam line at the European Synchrotron Radiation Facility and to D. Detollenaere and A.A. Snigirev for assistance and technical support in the experiment, as well as to the Swiss–Norwegian Beam Lines (SNBL) at the European Synchrotron Radiation Facility for the possibility of the measurements within the framework of the DUBBLE–SNBL internal agreement.

REFERENCES

1. *Great Soviet Encyclopedia* (Sov. Entsiklopediya, Moscow, 1973) [in Russian].
2. J. V. Sanders, Nature **204**, 1151 (1964).
3. J. V. Sanders, Acta Cryst. A **24**, 427 (1968).
4. J. V. Sanders, Acta Cryst. A **32**, 334 (1976).
5. E. A. Monroe, D. B. Sass, and S. H. Cole, Acta Cryst. A **25**, 578 (1969).
6. E. Yablonovitch, Phys. Rev. Lett. **58**, 2059 (1987).
7. S. John, Phys. Rev. Lett. **58**, 2486 (1987).

8. J. D. Joannopoulos, R. D. Meade, and J. N. Winn, *Photonic Crystals: Molding the Flow of Light* (Princeton Univ. Press, Princeton, 1995).
9. H. Miguez, C. Lopez, F. Meseguer, et al., App. Phys. Lett. **71**, 1148 (1997).
10. P. Jiang, J. F. Bertone, K. S. Hwang, and V. L. Colvin, Chem. Mater. **11**, 2132 (1999).
11. D. J. Norris, E. G. Arlinghaus, L. Meng, et al., Adv. Mater. **16**, 1393 (2004).
12. A. L. Rogach, N. A. Kotov, D. S. Koktysh, et al., Chem. Mater. **12**, 2721 (2000).
13. L. Meng, H. Wei, A. Nagel, et al., Nano Lett. **6**, 2249 (2006).
14. J. Hilhorst, V. V. Abramova, A. Sinitskii, et al., Langmuir **25**, 10408 (2009).
15. H. Wei, L. Meng, Y. Jun, and D. J. Norris, App. Phys. Lett. **89**, 241913 (2006).
16. A. van Blaaderen and P. Wiltzius, Science **270**, 1177 (1995).
17. J. H. J. Thijssen, A. V. Petukhov, D. C.'t Hart, et al., Adv. Mater. **18**, 1662 (2006).
18. Yu. A. Vlasov, V. N. Astratov, A. V. Baryshev, et al., Phys. Rev. E **61**, 5784 (2000).
19. R. Rengarajan, D. Mittleman, C. Rich, and V. Colvin, Phys. Rev. E **71**, 016615 (2005).
20. A. V. Petukhov, D. G. Aarts, I. P. Dolbnya, et al., Phys. Rev. Lett. **88**, 208301 (2002).
21. A. V. Petukhov, J. H. J. Thijssen, D. C.'t Hart, et al., J. App. Cryst. **39**, 137 (2006).
22. M. Kobas, T. Weber, and W. Steurer, Phys. Rev. B **71**, 224205 (2005).
23. T. R. Welberry, *Diffuse X-ray Scattering and Models of Disorder* (Oxford Univ., Oxford, 2004).
24. J. W. Goodwin, J. Hearn, C. C. Ho, and R. H. Ottewill, Coll. Pol. Sci. **252**, 464 (1974).
25. A. Snigirev, V. Kohn, I. Snigireva, and B. Lengeler, Nature **384**, 49 (1996).
26. W. Loose and B. J. Ackerson, J. Chem. Phys. **101**, 7211 (1994).
27. A. Guinier and G. Fournet, *Small-Angle Scattering of X-Rays* (Wiley, New York, 1955).
28. H. Versmold, Phys. Rev. Lett. **75**, 763 (1995).
29. A. J. C. Wilson, Proc. R. Soc. London Ser. A **180**, 277 (1941).
30. S. E. Paulin, B. J. Ackerson, and M. S. Wolfe, Phys. Rev. E **55**, 5812 (1997).
31. C. Dux and H. Versmold, Phys. Rev. Lett. **78**, 1811 (1997).
32. T. Sawada, Y. Suzuki, A. Toyotama, and N. Iyi, J. J. App. Phys. P.2 40, L1226 (2001).
33. R. M. Amos, J. G. Rarity, P. R. Tapster, et al., Phys. Rev. E **61**, 2929 (2000).

Translated by R. Tyapaev